

# Considerations for Dependability of the Motor Protection on Current Transformers Performance in VFD Applications

Umar Khan

Member, IEEE  
GE Grid Solutions  
Markham, ON, L6C 0M,  
Canada  
Umarnaseem.khan@ge.com

Iliia Voloh

Senior Member, IEEE  
GE Grid Solutions  
Markham, ON, L6C 0M,  
Canada  
[Iliia.voloh@ge.com](mailto:Iliia.voloh@ge.com)

Patrick Robinson

Associate Member, IEEE  
Altelec Eng. Services  
Calgary, AB, T2E 6Z2  
Canada  
pat@altelec.net

**Abstract** -- When generators or motors are started via variable frequency drive (VFD), initial frequency is very low, on the order of few hertz, and can be low for a considerable amount of time or even permanently. It is not well recognized in the industry about the consequences of low frequency on current transformers (CTs) performance and how this affects the protection performance as well. First, CTs are designed to operate at the nominal system frequency, however, when operating at low frequency, CTs could saturate at much lower currents, this can happen even at CT nominal current. Secondly, there are limits of the system frequency measurements in the protective relays, which will impact the correct current magnitude estimation and therefore the accuracy of the protection. And lastly, protective relays need full power-cycle to measure current; power-cycle will be considerably longer at lower frequency, therefore affecting fault clearance time.

This paper will educate engineers on how to consider CTs and protective relay's performance at lower frequencies to ensure adequate protection. It will also explore other solutions to address impact of the low frequency on the CTs and protection.

**Index Terms**--Current Transformer, Current Transformer Saturation, Motor Protection, Differential Protection, Overcurrent Protection, Variable Frequency Drive, Adjustable Speed Drive (ASD)

## I. INTRODUCTION

Variable frequency drives (VFDs) or adjustable speed drives (ASDs) have been widely used in the industry to achieve the desired mechanical output of the motor by controlling the voltage and frequency of the motor supply. Large electric motors, when started directly from the main power supply, draw high starting current resulting in voltage dips and overheating of the rotor part. In such applications, VFD is used as a soft-starter to prevent heating due to excessively large starting current and voltage dips. By controlling the supply frequency while maintaining the flux to its rated value (V/Hz constant), desired acceleration and rotational speed are achieved using the VFD.

When VFD is used as a soft-starter, it starts the motor from low speed (frequency) and accelerates to the desired speed level (off-nominal or rated). Rate of change of speed or acceleration/deceleration time from one level to another is normally programmable in most of the modern VFDs. For

example, VFDs allow programming of the total time required to accelerate from 0 to 60Hz in a range from 1 sec to 3000sec in MV drives and 1 to 6000sec in LV drives. Although the drive can accelerate the motor with the defined rate, the motor or application may not accept such rates. If the accelerating time is set too low, then the motor may draw too high current such that the overcurrent protection built-in the drive or motor relay may trip. The speed range of VFD fed motor is normally defined as a part of its rating [1]. Fig. 1 illustrates the current and frequency of the motor driven by the VFD.

This paper, previously presented in a conference [2], is reviewing the challenges associated with the performance of CTs and multifunctional relays when applied to low frequency applications such as VFD driven motor applications. Current transformers are designed to operate at system frequency 50Hz or 60Hz. Over a frequency range near the nominal operating frequency of the CT, the current transformer accurately replicates the primary currents to the secondary side of the CT [3]. However, magnetizing inductance is frequency dependent, as frequency decreases; the magnetizing coil impedance also decreases, resulting in the increase in the flux density and hence saturation of the core. Consequently, reliable operation of the motor protection relay can be jeopardized due to CT errors because of the de-rated CT excitation characteristic at low frequency currents. This paper intends to provide insight into CT performance at low frequencies so that improved performance of the relay can be achieved.

Section II reviews the basic magnetics of the current transformer. It reviews and explains (1) basic working

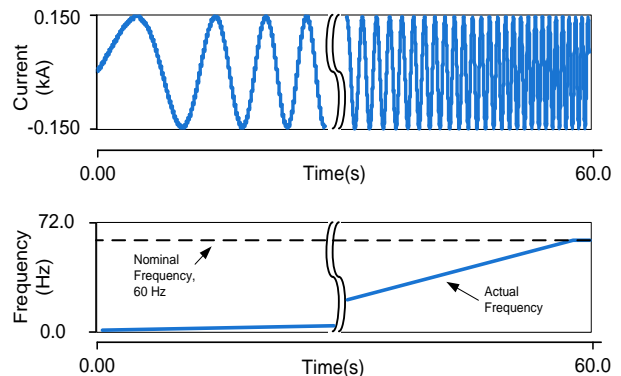


Fig. 1 Example of Motor Starting Current and Change in Frequency

principle of the CT, (2) fixed frequency analysis, (3) frequency dependent CT model and (4) excitation characteristic dependency on frequency.

Section III analyzes the impact of low frequency currents on the performance of the CT. For this purpose, frequency dependent current transformer model is used as well as real CT. The theoretical model of Section II is used to produce the frequency dependent CT excitation characteristic. To verify the frequency dependent model, performance of the CT at low frequency currents is tested using the real CT in the laboratory. This helps us to validate and verify the relevance of the theoretical CT model with the real CT. This section also explains: phasor measurement errors in the motor protection due to varying frequency challenges and their solutions associated with motor protection when applied to the low frequency motor operation.

## II. MAGNETICS OF THE CURRENT TRANSFORMER

Basic principles related to current transformers are reviewed first to develop the frequency dependent CT model for the analysis purposes.

### A. Excitation Characteristics

First, it is important to discuss the CT excitation characteristic and its key parameters prior to establish the current transformer saturation model. Fig. 2 shows a CT excitation characteristic. This curve illustrates the behavior of magnetic flux density,  $B$  (units Tesla) as a function of magnetic field,  $H$  (units Ampere-turns), also known as  $B$  vs  $H$  curve. Converting the magnetic analogies to electrical,  $B$  vs  $H$  curve can be represented as a secondary side excitation voltage ( $V_e$ ) and secondary side excitation currents ( $I_e$ ), also known as  $V_e$  vs  $I_e$  curve.

As illustrated by the Fig. 2, the curve shows two regions of CT operation, linear and non-linear. In the linear region, slope of the curve is greater than 1 and slope is less than 1 in the non-linear region. Three points are normally required to define the curve: knee point ( $V_K, I_K$ ), normal operating point below the knee point ( $V_n, I_n$ ) and above the point ( $V_s, I_s$ ). The knee point voltage when applied to the secondary terminals of the current transformer, which, when increased by 10%, will result in an increase of the exciting current by 50% [3]. Excitation voltage,  $V_s$  is the voltage required to develop 10A secondary excitation

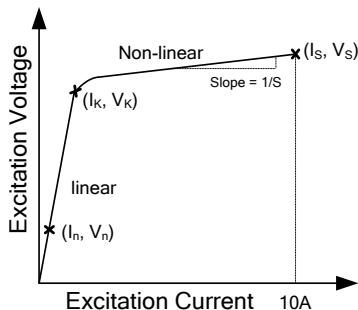


Fig. 2 Current Transformer Excitation Characteristics

current  $I_s$ . These points can be obtained from the excitation curve of the current transformer.

In the linear region, a CT operates as an ideal current transformer, transforming primary to secondary as per the turn ratio. In the non-linear region, as the excitation or magnetizing current increases, the CT enters the non-linear part of the characteristic, resulting in saturation of the transformer. When the CT saturates, it requires high excitation current to magnetize the core. More of the primary current is now used to magnetize the CT than to run the load current. Consequently, the secondary current of the CT becomes distorted.

### B. Equivalent Circuit of the Current Transformer

For protection studies, a simplified circuit diagram as shown in Fig. 3. The magnetizing branch is located on the secondary side and is represented with a non-linear inductor  $L_{mag}$ .

Using the circuit of Fig. 3, the equivalent circuit equation can be derived as below:

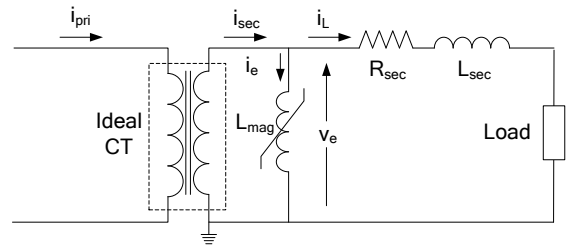
$$v_e(t) = i_L(t)R + L_{sec} \frac{di_L(t)}{dt} \quad (1)$$

where  $R = R_{sec} + R_{load}$

We can write the currents distribution equation per Kirchhoff's Current Law in the CT secondary circuit as follows:

$$i_{sec}(t) = i_e(t) + i_{load}(t) \quad (2)$$

Non-linear nature of the excitation current as a function of flux linkage or excitation voltage is developed based on the saturation model presented in [4]. Various approaches are available in literature to establish the non-linear behavior of the CT magnetic characteristic [11]. IEEE PSRC [4] presents a simplified saturation model of the CT, this paper uses this model for simulation purposes, which has been validated with the real current transformers in the laboratory tests. According



- $R_{sec}$ : secondary winding resistance
- $i_{pri}$ : primary winding current
- $L_{sec}$ : secondary winding inductance
- $i_{sec}$ : secondary winding current
- $L_{mag}$ : magnetizing inductance
- $i_e$ : magnetizing branch current
- Load: relay load
- $i_L$ : secondary winding current
- $v_{mag}$ : voltage across magnetizing branch

Fig. 3 Equivalent Circuit Diagram of the Current Transformer

to Faraday's law, change in flux must change the voltage ( $v_e$ ) across the magnetizing branch. The relation between the voltage and flux can be written as:

$$v_e(t) = N \frac{d\Phi(t)}{dt} \quad (3)$$

For a sinusoidal voltage, flux is also sinusoidal

$$\Phi = \Phi_{max} \cdot \sin(2\pi ft) \quad (4)$$

Replacing  $\Phi$  in (3) with (4):

$$v_e(t) = N \frac{d\Phi_{max} \cdot \sin(2\pi ft)}{dt} \quad (5)$$

$$v_e(t) = 2\pi f \cdot N \cdot \Phi_{max} \cdot \cos(2\pi f \cdot t) \quad (6)$$

Using (4),  $\Phi_{max}$  can be written as

$$\Phi_{max} = V_{e\ max} \frac{1}{2\pi f \cdot N} \quad (7)$$

where,  $f$  is the signal input frequency;  $N$  is the turns ratio and  $V_{e\ max}$  equals  $\sqrt{2}V_e$

### C. Laboratory Test Bench

A real typical MV motor current transformer having excitation curve shown in Fig. 4 and CT data in Table I, is used to validate the frequency dependent model of Section IID. As shown in Fig. 4, the saturation point is graphically calculated by taking the cross point of the straight lines of the excitation curve [12]. V-I curve is measured for the nominal (60Hz) and off-nominal (40, 20, 10, 5Hz) motor operating frequencies. Secondary excitation test method [5] is used to establish the frequency dependent V-I curve of the current transformer. With the primary circuit open, varying voltage is applied at the CT secondary terminals and the current in the secondary winding is measured at each level of the applied voltage. Fig. 5 shows the excitation test circuit and laboratory test bench used for the V-I measurements.

### D. Development of The Frequency Dependent CT Model

To study and analyze the behavior of CT at low frequency currents, it is important to model the frequency dependent excitation characteristic (V-I or  $\phi$ -I) of the magnetizing branch. As we know, the core of the CT is designed for a uniform flux density ( $B$ ) at given volts per turn at constant frequency. Such that voltage ( $B_{max}$ ) can be defined as a function of flux density ( $V_e$ ), cross-sectional area of the core ( $A_{core}$ ) and frequency:

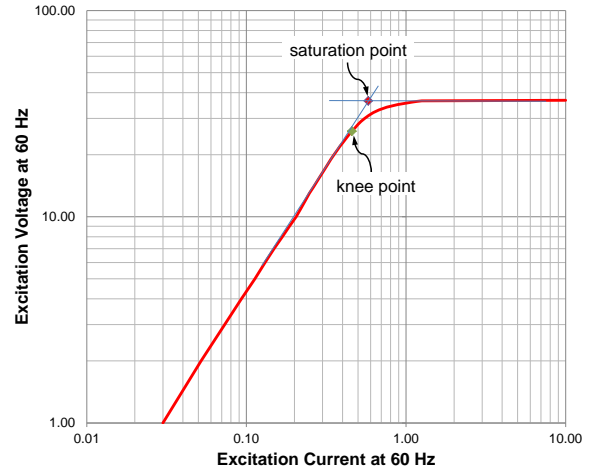


Fig. 4 Measured Excitation Characteristic of Class C20 Current Transformer with Turn Ratio 100:5

$$B_{max} = \frac{V_e}{4.44 f \cdot N \cdot A_{core}} \quad (8)$$

Equation (8) suggests that when the magnetic circuit is excited by the sinusoidal voltage, the ratio between the voltage and frequency must be kept constant to establish a uniform flux density. Over- or under excitation of the magnetic core will happen, if frequency is changed above/below the allowable limit without changing the voltage. Magnetizing inductance is frequency dependent, as frequency decreases; the magnetizing coil impedance also decreases resulting in the increase of the flux density and hence the saturation of the core.

A CT having excitation curve shown in Fig. 4 and CT data in Table I, is used as an example for the analysis purposes:

Based on (6), flux density must be kept constant to operate the CT in the allowable excitation limits. If the CT is operated at low frequency, then voltage must be reduced such that flux

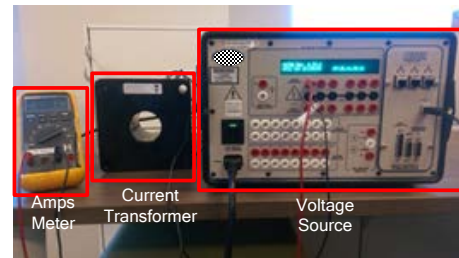
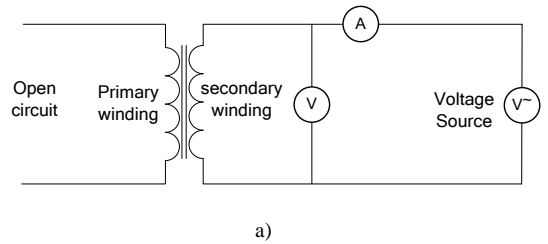


Fig. 5 (a) Excitation Test Circuit, (b) Excitation Test Bench

TABLE I  
CT DATA  
Required Data

Required Data	
Relay Class	C20
Turn ratio	100:5
Frequency	60Hz
Secondary winding resistance ( $R$ )	0.062 $\Omega$
Voltage ( $V_s$ ) at 10A excitation current	36.7V
Slope ( $S$ )	2.5%
Knee point voltage ( $V_{knee}$ )	26V
Saturation Voltage ( $V_{Sat}$ )	36.5V

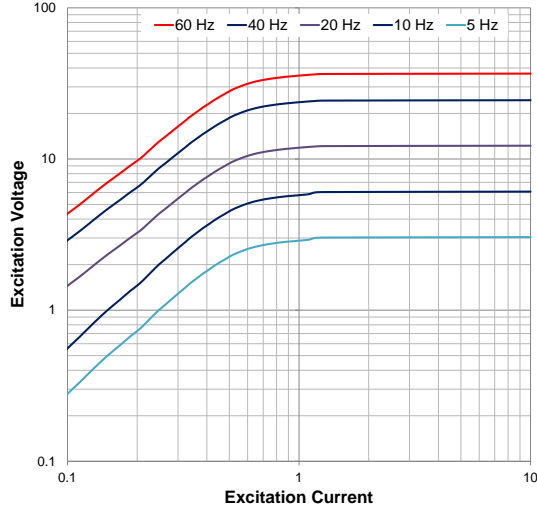


Fig. 6 Measured V-I Characteristic for 60, 40, 20, 10 and 5 Hz Motor Operating Frequencies

density remains uniform. Using this fact, saturation characteristic of the CT can be estimated at the low frequencies.

For example: using the data of Table I in (7), calculated peak flux linkage equals  $6.87 \times 10^{-3}$  Wb-turns. When motor-fed-through-VFD is running at 20Hz frequency, peak flux density of  $6.87 \times 10^{-3}$  Wb-turns will be developed when peak excitation voltage  $V_s (=V_{e\max})$  equals 12.22V.

Fig. 6 shows the V-I curve measured using the laboratory test bench (shown in Fig. 5). It is evident from the Fig. 6 that when the frequency is 20Hz, voltage required to produce the same flux density is now reduce by the factor below:

$$V(@F) = V(@F_n) \cdot \frac{F}{F_n} \quad (9)$$

where  $F_n$  is the nominal frequency and  $F$  is the actual motor input frequency.

Hence when the frequency is 20Hz the voltage must be equal to 12.22V to develop the required flux density. Table II shows de-rated CT data for operating frequency 40, 20, 10 and 5Hz.

### III. SIMULATION RESULTS AND IMPACT TO PROTECTION RELAYS

Proper operation of the relay is largely influenced by the CT performance. If properly selected, under normal steady state conditions, a CT operates in its linear part of the excitation curve (Fig. 2). However, short circuit current can be steady state (purely AC) or transient (DC component in the fault current) in nature. For the short circuit analysis, in addition to off-nominal low frequency, the other factors that influence the CT performance are effective burden on CT terminals, magnitude and duration of the DC component in the fault current and residual flux. In VFD motor applications, low frequency operation influences the CT performance and hence operation of the protection relays.

TABLE II  
DE-RATED CT DATA

	60Hz	40Hz	20Hz	10Hz	5Hz
Relay Class	C20				
Turn ratio (N)	100:5				
Secondary winding resistance (R)	0.062Ω				
Voltage ( $V_s$ ) at 10A excitation current	36.7V	24.4V	12.3V	6.1V	3.05V
Knee point Voltage ( $V_{knee}$ )	26V	17.33V	8.66V	4.33V	2.16V
Saturation Voltage ( $V_{Sat}$ )	36.5	24.33V	12.16V	6.08V	3.04V

Frequency dependent saturation model established in section II and laboratory measurements of V-I current is used to model the CT for simulation purposes. Important parameters considered for analysis purposes are:

- Effective burden on CT terminals:  $0.37\Omega$ , which includes Relay  $0.008\Omega$  [6], CT lead  $0.3\Omega$  (AWG 8 and loop length of 145 meters) and CT winding resistance  $0.062\Omega$ .
- X/R ratio of 15 for a motor rating of 440HP, 2.3kV, 60Hz and service factor (SF) of 1.15 and power factor of 0.87 at 100% load.

Performance of the CT during all the above-mentioned motor steady state operating conditions and short circuit conditions are further analyzed and discussed as follows:

#### A. Motor Load Conditions

Maximum allowable motor loading condition is defined by the parameter *Service Factor* (SF) provided in the motor data sheet. To load a motor in its thermal limits, maximum loading is limited by the multiple of SF. For example: for the motor under consideration having rated HP of 440 (full load amps, FLA, 82A) and SF=1.15, the maximum allowable loading of the motor is limited to 440HP x 1.15 (506HP or 94A).

At the maximum allowable loading condition, motor draws 94A (FLA x SF), current transformer operates in the linear region for all input frequency levels.

Linear operating range of the current transformer, under test, can be calculated using information available in Table II. Up to this range, excitation current is negligible (0.6A when CT is operating at nominal frequency).

Note: Motor under normal running load conditions with very low operating frequencies, as shown in Table II, are not the practical cases. Authors used these values for example purposes. However, under short circuit or non-steady state conditions when VFD driven motor is in the starting mode of

TABLE III  
MAXIMUM ALLOWABLE BURDEN CURRENT

	60HZ	40Hz	20Hz	10Hz	5Hz
Effective burden at CT terminals( $R_{eff}$ )	0.37Ω				
Saturation Voltage ( $V_{Sat}$ )	36.5V	24.33V	12.16V	6.08V	3.04
Saturation Current ( $I_{Sat}$ )	1973A	1315A	657A	329	164A

operation, consideration of the low frequencies is important when analyzing CT and relay performances.

For example, when the input frequency is 60Hz, the maximum primary current level (reference level), above which CT enters the saturation zone, equals 1973A. Similarly, reference level of off-nominal low frequencies is calculated as shown in the Table III. Maximum allowable motor loading is well below the reference level and therefore, excitation current is negligibly small and lies in the linear part of the excitation curve. It can also be observed that reference level decreases as the operating frequency decreases.

### B. Locked-Rotor Condition

During locked-rotor condition, the motor current may reach or exceed seven times the rated full load current [7]. Rotor condition may not be a concern in motor applications when the motor is driven by a VFD due to the reason that VFD confines motor operation to its torque speed characteristic during motor starting and running conditions [8].

### C. Short Circuit Condition

Current during short circuit can be significantly higher than the rated full load amps. As mentioned earlier, short circuit can be steady state or transient in nature. We will analyze both states in detail.

**Steady State Short Circuit:** Steady state short circuit current is purely AC in nature without DC component. Therefore, current level above the reference level  $I_{Sat}$ , as determined in Table III, will result in saturation of the current transformer.

Fig. 7 illustrates the sinusoidal waveforms and the magnitudes of the secondary currents at different operating frequencies. Short circuit is purely AC in nature with magnitude of 820A RMS on CT primary. As can be seen in Fig. 8, the short circuit current (1000A) is below the reference level 1973A and 1315A for 60Hz and 40Hz, respectively, therefore, secondary of the CT is undistorted. However, short circuit current (1000A) is above the reference level 657 and 329A, therefore, CT, operating at 20 and 10Hz, has distorted secondary current, which is significantly distorted at 10Hz.

In VFD motor application, in order to avoid CT saturation in steady state short circuit conditions, lowest operating frequency must be considered when specifying CTs. Assuming a lowest operating frequency is  $F_m$ , CT saturation voltage level must satisfy the following relation to avoid saturation when operating at  $F_m$ :

$$V_{Sat}(@60hz) > \frac{I}{TurnRatio} \times R_{eff} \times \frac{F_n}{F_m} \quad (10)$$

where  $R_{eff}$  is the effective impedance at CT secondary terminals,  $F_n$  is the nominal frequency and  $F_m$  is the lowest operating frequency in the VFD motor application.

**Transient Short Circuit:** Transient or asymmetrical current contains decaying DC component in addition to AC component. Magnitude and duration of the decaying DC component depends on the system X/R ratio and fault inception point referenced to the voltage signal (known as Point-on-Wave POW). Fig. 8 illustrates the signatures of secondary currents when the CT is operating at 60, 40, 20 and

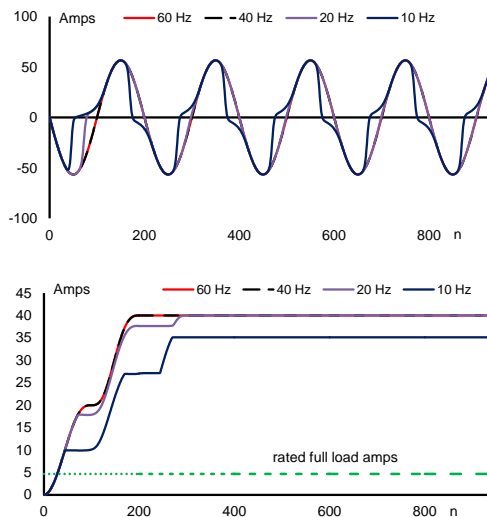


Fig. 7 Sinusoidal and RMS Measurement of the Steady State Short Circuit Secondary Current

10Hz while the short circuit current is transient in nature with an AC magnitude of 300A RMS at CT primary. It can be observed that the DC component magnifies the total asymmetrical current to more than 800A, resulting in saturation of the current transformer for all frequency levels.

In VFD motor application, in order to avoid CT saturation in transient short circuit conditions, CT saturation voltage level must satisfy the following relation [9] to avoid saturation when operating at  $F_m$ :

$$V_{Sat}(@60hz) > \frac{I_F}{TurnRatio} \times R_{eff} \times \left(1 + \frac{X}{R}\right) \times \frac{F_n}{F_m} \quad (11)$$

### D. Impact on Protection Relays

Multifunctional protection relays experience various challenges and issues when applied to low frequency input

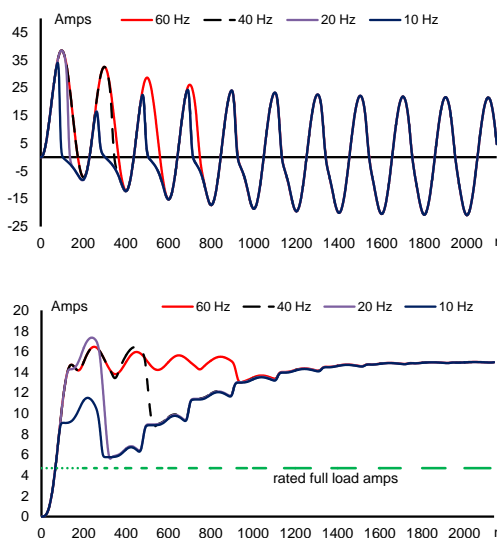


Fig.8 Sinusoidal and RMS Measurement of the Steady State Short Circuit Secondary Current

signals. Today's relays not only offer protection but incorporate monitoring and control functions as well. Therefore, protection as well as monitoring functions must be considered when applying the low frequency input signals.

The above analysis shows that a CT is more likely to saturate as the frequency decreases from the nominal frequency, which could impact the performance of the protection functions. However, the impact of low frequency is not just limited to CT saturation but also impacts phasor measurements, metering and monitoring elements.

As mentioned in the Section I, in VFD applications, the frequency of the motor input current signals during starting varies from low frequency to the desired frequency level with a defined rate of change. Moreover, some applications require the motor to run at off-nominal frequency (speed) during the normal load conditions. Therefore, depending on the motor running condition, measurement error varies with the varying frequency.

Fig. 9(a) demonstrates the magnitude estimation of the motor starting current using root-mean-square (RMS) and discrete Fourier transformer (DFT) techniques having a fixed sampling frequency of 3840Hz and nominal frequency of 60Hz (sampling rate  $N$  equals 64samples/cycle). It shows a significant error in the measurement which decreases as the frequency approaches the nominal frequency level. This is because with the fixed sampling frequency, samples per cycle changes as frequency changes which results in the measurement error. For example, for a nominal frequency of 60Hz,  $N$  equals 64 samples in one cycle ( $F_s=3840\text{Hz}$ ) and for a frequency 50Hz,  $N$  will increase to 77 samples in one cycle, due to the change in the window length. Hence, using estimation techniques with a fixed sampling frequency will not provide a correct estimation of the phasors of a varying frequency input signal.

Typically, RMS- or DFT-type estimators are used to calculate phasors for the current based short circuit protection functions of modern microprocessor based relays. Because DFT extracts only the fundamental component of the input signal, it results in a lower estimate of the magnitude of input signals. The actual cause of the lower estimation of the magnitude using DFT-type, compared to RMS-type, is varying frequency. If there is no frequency tracking available, DFT-type calculates the lower magnitude than RMS-type estimator (see Fig. 9(a))

Current based short circuit protection elements that use DFT-type phasors to detect the presence of higher levels of fault currents will be affected. This issue can be solved by using the RMS-type estimator complemented with a peak sample detector to detect the maximum fault current level, but such estimator accuracy will not be great.

Using tracking frequency to adjust the sampling frequency of the phasor estimators helps to achieve correct measurement of the varying frequency input signals. As shown in Fig. 9(b), magnitude of the input signal still shows measurement error in the first few cycles. RMS magnitude shows large oscillations in measurement while DFT magnitude shows calculation delay until magnitude reaches the actual magnitude level.

This issue can be solved if frequency tracking is forced to initialize at a defined frequency level known as "Starting Frequency,  $F_{start}$ " instead of nominal frequency. As soon as a motor starts, the sampling rate is adjusted as per the set starting frequency instead of nominal frequency until frequency tracking starts providing the real frequency. This feature will help to reduce the measurement error significantly by forcing reduction of the difference ( $\Delta F$ ) between the estimated and real frequency.

For example, in the application of a motor fed through a VFD that starts at frequency of 10Hz, the relay engineer must use the Starting Frequency feature and program the starting frequency value to 10Hz.

Undercurrent protection typically uses fundamental currents (DFT-type) to detect loss of load or undercurrent operating conditions of the motor. However, it is important to block the undercurrent protection during motor starting. The reason is: during motor starting, the current magnitude measurement (DFT-type) may remain below the undercurrent threshold for some duration of time until the current reaches the undercurrent threshold level. Duration of block time depends on the provision of tracking frequency.

Differential protection performance during an external fault: Single- or dual-slope characteristic and higher pickup are typically used to prevent mal-operation of the differential protection in the event of an external fault with CT saturation. However, it won't impact the differential operation because both ends CTs see the same low frequency currents resulting in zero or very small false differential current measurement.

Differential protection performance during internal fault: However, in the case of an internal fault terminal CTs will see a high fault current. Differential protection must now operate to isolate the motor from the system. However, when VFD fed

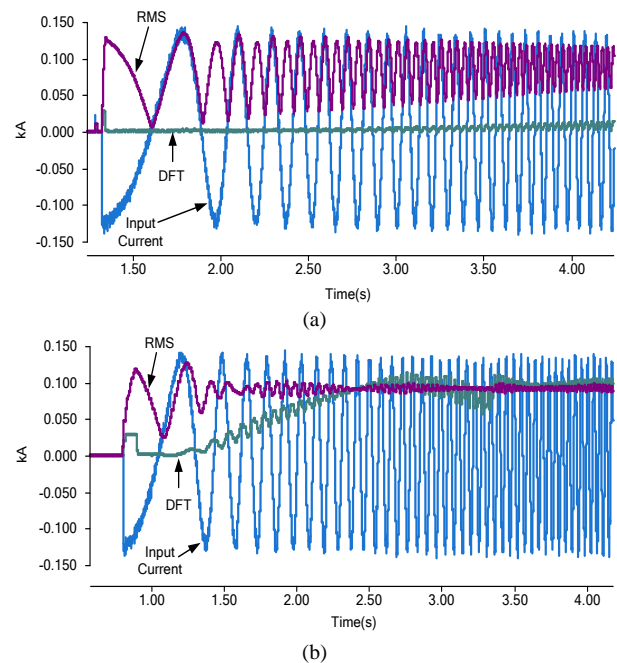


Fig. 9 Magnitude Estimation Using (a) Fixed Sampling Frequency (b) Adjusted Sampling Frequency

motor is operating at low frequency, fault current can saturate the CT if not properly selected, as discussed in section III C. Operation of the differential protection may be in jeopardy, if differential is set not too sensitive.

Overcurrent protection can be affected by the VFD motor application when motor is running at low speed or low frequency. Fig. 10 shows that when CT is properly selected considering low frequency into account (as discussed in section III D) overcurrent correctly operates as soon as the primary current reaches the pickup level. However, in case of CT saturation, secondary current doesn't replicate the primary current and reaches the pickup level after 33msec, resulting in the delayed operation of the overcurrent, which can result in the severe damage to the motor as energy accumulation in the low frequency currents is significantly very large compared to higher frequency.

This problem can be solved by (1) proper selection of current transformer (2) lower setting of the overcurrent pickup level, care must be taken that overcurrent must be selected about the maximum allowable load current that equals  $SF \times FLA$ .

Many of the today's digital relays provide multi setpoint groups; when required protection, settings can be switched to different settings for a different operating condition [6]. In VFD motor applications having prolonged low frequency motor operation, adjustment to the protection settings can be achieved by automatic switching between groups at different frequency levels.

#### IV. CONCLUSIONS

This paper discussed multifunctional motor protection relay performance dependability on current transformer in VFD driven motor applications.

Current transformers are normally designed to operate at the nominal system frequency 50Hz or 60Hz. In variable speed drive motor applications having prolonged low frequency motor operation; this can result into saturation of the CT. As the frequency decreases, the voltage across the CT magnetizing branch decreases as well to maintain the flux density. Thus, CT excitation characteristic is now de-rated to lower level. Consequently, reliable operation of the motor protection relay can be jeopardized with CT saturation happening at low frequency currents even at low level currents.

Low off-nominal frequency motor operation not only de-rate the CT excitation characteristic, but results in significant increase of the phasor measurement error in the relay, if there is no proper frequency tracking.

At low frequency operation, it is likely that CT saturates during the short circuit condition, it is highly recommended to lower the pickup settings of overcurrent protection and block undercurrent relay during motor start. In an event of an external fault with CT saturation, differential protection remains secure. Proper differential protection operation during external/internal with CT saturation can be achieved using the CT saturation detection technique complement with fault direction.

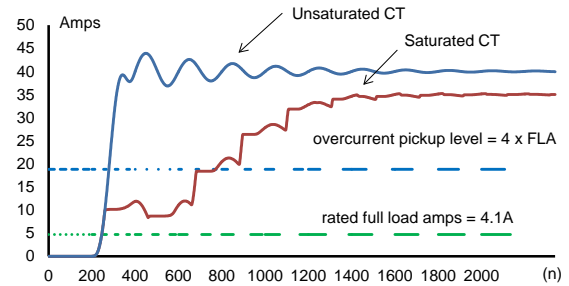


Fig. 10 Sinusoidal and RMS Measurement of the Steady State Short Circuit Secondary Current

#### V. REFERENCES

- [1] NEMA, Application Guide for AC Adjustable Speed Drive Systems, Rosslyn, VA.
- [2] U. Khan, I. Voloh and P. Robinson, "Considerations for Dependability of the Motor Protection on Current Transformers Performance in VFD Applications," *2016 Petroleum and Chemical Industry Technical Conference (PCIC), Philadelphia, PA, 2016*.
- [3] IEC Instrument transformers – Part 2: Additional requirements for current transformers, IEC Standard 67869-2, September 2012.
- [4] Working Group Report of the IEEE Power System Relaying Committee, CT SAT Calculator, [http://www.pes-psrc.org/Reports/CT\\_SAT%2010-01-03.zip](http://www.pes-psrc.org/Reports/CT_SAT%2010-01-03.zip), 2003.
- [5] IEEE Std C57.13.1-1981, *Field Testing Relaying CT*
- [6] Instruction Manual, 869 Motor Protection System, GE Digital Energy, 2014.
- [7] IEEE C37.110-2007, IEEE Guide for the Application of Current Transformers Used for Protective Relaying Purposes.
- [8] Application Guide for AC Adjustable Speed Drive Systems NEMA Standards Publication.
- [9] Z. Xu, M. Proctor and I. Voloh, "CT Saturation Tolerance for 87L Applications" in *Proc 68th Annual Conference for Protective Relay Engineers, Texas A&M, March 30 - April 02, 2015*.
- [10] R. Hunt, L. Sevov and I. Voloh, "Impact of CT Errors on Protective Relays - Case Studies and Analysis," in *Proc. the Georgia Tech Fault & Disturbance Analysis Conference, May 19-20, 2008*.
- [11] Working Group C-5 of the Systems Protection Subcommittee of the IEEE Power System Relaying Committee, "Mathematical Models for Current, Voltage, and Coupling Capacitor Voltage Transformers," IEEE Transactions on power delivery, vol. 15, no. 1, pp. 62-72, January 2000.
- [12] IEEE Guide for the Application of Current Transformers Used for Protective Relaying Purposes, IEEE Standard C37.110-2007, April 2008.

#### VI. VITAE

**Umar Khan** (M'08) received his B.E. degree from Ghulam Ishaq Khan Institute (GIKI), Pakistan, in 2005, and M.Sc. degree from Wroclaw University of Technology, Wroclaw, Poland, in 2009, and a Ph.D. degree in electrical power system from University of Western Ontario, Canada, in 2013. Since 2013, he is working with GE Digital Energy, Canada. His current areas of interest are power system protection, control, and monitoring.

**Iliia Voloh** (SM'99) received his Electrical Engineering degree from Ivanovo State Power University, Russia. He is currently an applications engineering manager with GE Digital Energy, Canada. His areas of interest are current protection algorithms and advanced communications for protective relaying. Iliia authored and co-authored more than 30 papers presented at major North America Protective Relaying conferences. He is an active member of the IEEE PSRC, a member of the main PSRC Committee and a senior member of the IEEE.

**Patrick Robinson** (M'95) graduated with honors from Electrical Engineering Technology at the Northern Alberta Institute of Technology in 1995. Since that time, he has worked in the fields of electrical protection and control with Altec Engineering Services